Flexural Strength and Ductility of Extended Pile-Shafts. I: Analytical Model

Y. H. Chai, M.ASCE[1]

Abstract: An analytical model, based on the commonly used equivalent cantilever concept, is developed for assessing the local ductility demand of a yielding pile-shaft when subjected to lateral loading. For elastic response of the pile-shaft, an equivalent depth-to-fixity is assumed, which can be derived by equating the lateral stiffness of the cantilever to that of the elastic soil-pile system. In adapting the equivalent cantilever model to yielding pile-shafts, however, the depth-to-maximum-moment is assumed to occur at a depth above the depth-to-fixity. The lateral strength, which depends on the depth-to-maximum-moment, is determined using the flexural strength of the pile and the ultimate pressure distribution of the soil. By assuming a concentrated plastic hinge rotation at the depth-of-maximum-moment, a kinematic model relating the local curvature ductility demand to global displacement ductility demand is developed. The kinematic relation is shown to depend on the aboveground height, depth-to-maximum-moment, depth-to-fixity, and equivalent plastic hinge length. The model is illustrated using a pile-shaft embedded in cohesive and cohesionless soils.

DOI: 10.1061/(ASCE)0733-9445(2002)128:5(586)

CE Database keywords: Flexural strength; Ductility; Concrete piles; Concrete, reinforced; Lateral loads; Models.

Introduction

Current seismic design of bridge structures is based on an assumed ductile response of the structure. A capacity design principle is generally followed to ensure that regions of inelastic deformation are carefully detailed to provide adequate structural ductility. Nonductile failure modes are suppressed by providing a differential strength between the ductile and nonductile failure modes. Regions outside of those with special detailings are protected from inelastic actions and hence prevented from potential brittle failures.

For most bridges, the foundation system may be strategically designed to remain elastic while the pier portion of the substructure is detailed for inelastic deformation and energy dissipation. This approach is intended to avoid the difficulty of post earthquake inspection and the high cost associated with repair of the damaged foundation. Elastic response of the foundation can be ensured by increasing the strength of the foundation above that of the bridge pier so that plastic hinging occurs in the pier instead of the foundation. However, many design situations arise where plastic hinging cannot be avoided in members of the foundation during a severe earthquake. A good example of such design is the extended pile-shaft, as shown in Fig. 1(a or b), where the column is continued below the ground level as a pile-shaft of approximately the same diameter. Such foundation design is cost-effective when compared to the column/pile-cap/pile combination since the construction of an expensive pile-cap can be eliminated. Under seismic loading, the maximum bending moment occurs in the pile at some distance below the ground level, depending on the relative stiffness between the pile and surrounding soil. The magnitude of the bending moment under the design level earthquake is often sufficiently large to cause plastic hinging of the pile. Consequently, the design of such foundation requires careful considerations of the flexural strength and ductility capacity of the pile.

In addition to the difficulty of damage inspection after an earthquake, extensive yielding of the pile below the ground level might result in an unacceptable level of residual displacement, which may render the structure unserviceable after an earthquake. In order to limit the yielding of the pile, and hence damage in the pile, the lateral strength of these members is currently prescribed at a level higher than that of an equivalent column. This approach attempts to ensure that the full ductility capacity of the pile will not be developed under the design level earthquake, even though full detailing requirements are imposed on the design of these members. Such structures have been termed as *Limited Ductility Structures* by ATC-32 (1996), where a displacement ductility factor of 3 has been implicitly prescribed for design. A similar approach of prescribing higher lateral strength for piles has been adopted for seismic design of highway bridges in New Zealand. For plastic hinges expected at a depth less than 2 m below the ground level but not below the mean water level, the design displacement ductility factor is limited to $\mu_\Delta \leqslant 4$. For plastic hinges expected at a depth greater than 2 m below the ground level or below the mean water level, the design displacement ductility factor is reduced to $\mu_\Delta \leqslant 3$ (Chapman 1995; Park 1998).

The lateral stiffness, strength, and ductility capacity of the pile depend on the amount and details of the longitudinal and transverse reinforcement, and to a lesser extent, the compressive strength of the concrete. The lateral force-deformation characteristics of the pile also depend on the interaction between the pile and surrounding soil. For most bridges, however, the inertial force from the superstructure tends to dominate the inelastic deformation of the pile. Consequently, the inelastic deformation of the

[1]Associate Professor, Dept. of Civil and Environmental Engineering, Univ. of California, Davis, CA 95616.

Note. Associate Editor: C. Dale Buckner. Discussion open until October 1, 2002. Separate discussions must be submitted for individual papers. To extend the closing date by one month, a written request must be filed with the ASCE Managing Editor. The manuscript for this paper was submitted for review and possible publication on June 6, 2000; approved on August 22, 2001 . This paper is part of the ***Journal of Structural Engineering***, Vol. 128, No. 5, May 1, 2002. ©ASCE, ISSN 0733-9445/2002/5-586–594/$8.00+$.50 per page.

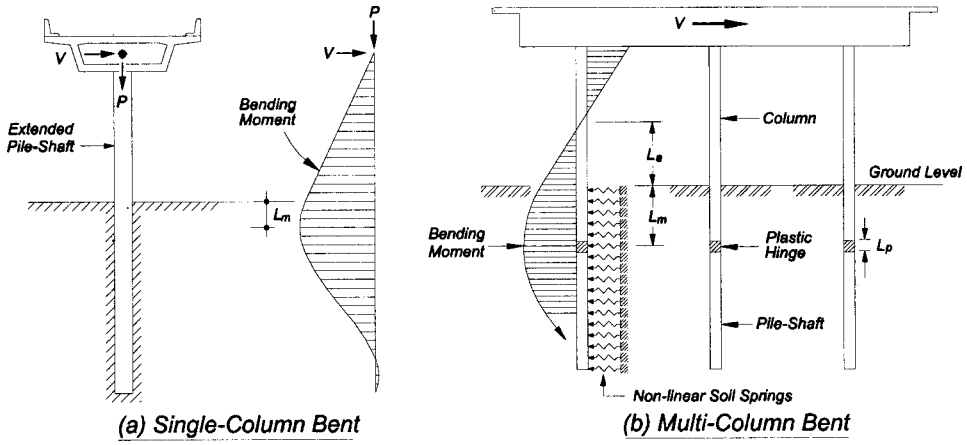

Fig. 1. Formation of subgrade plastic hinge due to inertial loading of superstructure

pile frequently occurs at a depth very close to the ground surface (typically less than three or four pile diameters below the ground surface). Exceptions to such shallow inelastic deformation include piles embedded in liquefiable soils or piles embedded in soil layers with large stiffness contrast where the pile may be subjected to a large local deformation due to kinematic loading, or in situations where the lateral spread of an adjacent soil mass may impose a large deformation on the pile. In this paper, only the inelastic response dominated by inertial loading is considered. An analytical model, based on an extension of the equivalent cantilever method, is developed for assessing the flexural strength and ductility capacity of reinforced concrete piles embedded in cohesive and cohesionless soils. Comparisons of the model with experimental test results are presented in a companion paper (Chai and Hutchinson 2002).

Equivalent Cantilever Model

Elastic Soil-Pile System

A common approach for structural design of a pile foundation assumes that the soil-pile system can be replaced by an equivalent cantilever that is fully restrained against lateral translation and rotation at the base, as shown in Fig. 2 (Caltrans 1986; Dorwick 1987). The equivalent depth-to-fixity, typically in the range of 3–6 pile diameters below the ground level, is used to account for the flexibility of the embedded pile. The equivalent depth-to-fixity depends on the relative stiffness between the pile and surrounding soil and may be determined by equating the lateral stiffness of the soil-pile system to that of an equivalent fixed-base cantilever.

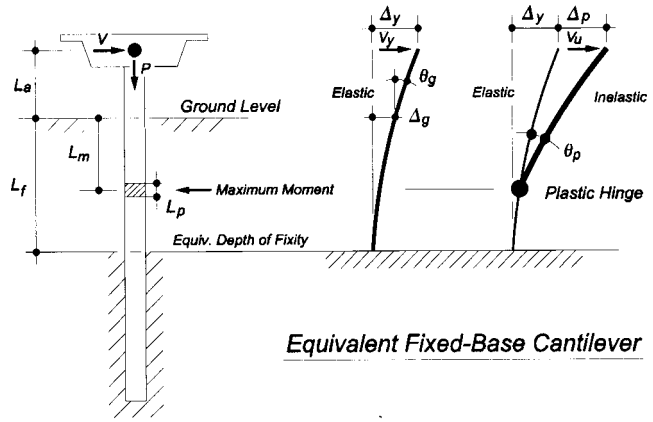

Fig. 2. Representation of soil-pile system by equivalent fixed-base cantilever

The elastic lateral stiffness of a prismatic equivalent fixed-base cantilever is given by

$$K_c \equiv \frac{V}{\Delta} = \frac{3EI_e}{(L_f + L_a)^3} \tag{1}$$

where V=lateral force applied at the top of the cantilever; Δ=lateral displacement at the top of the cantilever; EI_e=effective flexural rigidity of the equivalent cantilever (assumed to be the same as that of the pile); L_a=aboveground height; and L_f=equivalent depth-to-fixity. For concrete piles, the flexural rigidity in Eq. (1) should account for the possible reduction of stiffness due to cracking of the concrete. In this case, the effective flexural rigidity EI_e may be taken as the secant stiffness of the pile section at first yield of the reinforcement. The equivalent depth-to-fixity L_f may be determined by equating the lateral stiffness of the equivalent cantilever to the lateral stiffness of the soil-pile system using known solutions for elastic piles embedded in an elastic Winkler foundation. The lateral stiffness of the soil-pile system and the equivalent depth-to-fixity will be determined separately for cohesive and cohesionless soils.

Equivalent Depth-to-Fixity: Cohesive Soils

For an elastic pile embedded in a cohesive soil, the lateral stiffness of the soil is commonly modeled with an elastic Winkler foundation with a constant modulus of horizontal subgrade reaction. The solution for an elastic pile embedded in a soil with a constant modulus of horizontal subgrade reaction is well known (Poulos and Davis 1980; Pender 1993). For a long pile, i.e., embeddment length greater than 3.5 times the characteristic length R_c [defined later in Eq. (4)], the lateral displacement Δ_g and rotation θ_g of the pile at the ground level are given by (Poulos and Davis 1980)

$$\Delta_g = \frac{V(L_a + \sqrt{2}R_c)}{k_h R_c^2} \tag{2}$$

$$\theta_g = \frac{V(\sqrt{2}L_a + R_c)}{k_h R_c^3} \tag{3}$$

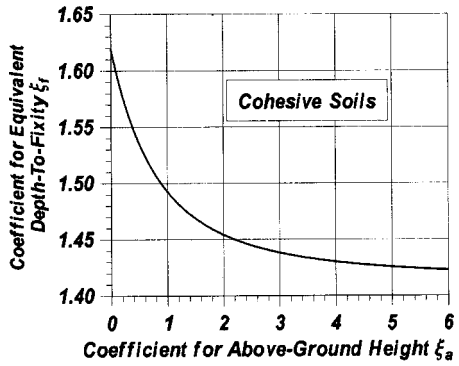

Fig. 3. Coefficient for equivalent depth-to-fixity of cohesive soils

where k_h=constant modulus of horizontal subgrade reaction in unit of force/length^2, and the characteristic length R_c is given by

$$R_c = \sqrt[4]{\frac{EI_e}{k_h}} \tag{4}$$

Note that the influence of axial force on ground level displacement and rotation of the pile has been ignored in Eqs. (2) and (3). The lateral displacement at the top of the pile consists of contributions from the lateral displacement and rotation of the pile at the ground level and the flexural deformation of the pile above the ground

$$\Delta = \Delta_g + \theta_g L_a + \Delta_{L_a} \tag{5}$$

where Δ_{L_a} corresponds to the flexural deflection of the pile above the ground and is given by

$$\Delta_{L_a} = \frac{VL_a^3}{3EI_e} \tag{6}$$

By defining the aboveground height L_a and equivalent depth-to-fixity L_f in terms of the characteristic length R_c, i.e., $L_a \equiv \xi_a R_c$ and $L_f \equiv \xi_f R_c$, where ξ_a and ξ_f=coefficients for the aboveground height and equivalent depth-to-fixity, respectively, the lateral stiffness of the soil-pile system can be written as

$$K_{\text{sp}} \equiv \frac{V}{\Delta} = \frac{3k_h R_c}{3\sqrt{2} + 6\xi_a + 3\sqrt{2}\xi_a^2 + \xi_a^3} \tag{7}$$

The coefficient for equivalent depth-to-fixity ξ_f can be obtained by equating the lateral stiffness of the soil-pile system K_{sp} from Eq. (7) to the lateral stiffness of the equivalent cantilever K_c from Eq. (1)

$$\xi_f = \sqrt[3]{4.24 + 6\xi_a + 4.24\xi_a^2 + \xi_a^3} - \xi_a \tag{8}$$

Note that the coefficient for equivalent depth-to-fixity ξ_f is only a function of the coefficient for aboveground height ξ_a in Eq. (8). The coefficient for equivalent depth-to-fixity, however, is not very sensitive to the aboveground height, particularly for large values of ξ_a. Fig. 3 shows the variation of the coefficient for equivalent depth-to-fixity for $0 \leqslant \xi_a \leqslant 6$. For $\xi_a = 0$, i.e., lateral load applied at the ground level, the coefficient for equivalent depth-to-fixity is $\xi_f = 1.62$. For $\xi_a > 0$, the coefficient for equivalent depth-to-fixity decreases rapidly with increase in the coefficient for aboveground height. For aboveground height in the range $1 < \xi_a < 6$, the coefficient for equivalent depth-to-fixity varies between 1.42 and 1.49. The relative insensitivity of ξ_f led to an approximate expression for the equivalent depth-to-fixity (Dorwick 1987; Scarlat 1996). For a free-head pile embedded in a cohesive soil and loaded with a horizontal force at an aboveground height of L_a, the equivalent depth-to-fixity has been given by Scarlat (1996) as

$$L_f = 1.4R_c \quad \text{if } L_a/R_c \geqslant 2 \tag{9}$$

$$= 1.6R_c \quad \text{if } L_a/R_c < 2 \tag{10}$$

Eq. (9) was suggested by Davisson (1970) earlier for $L_a/R_c \geqslant 2$.

The equivalent depth-to-fixity L_f can be calculated if the modulus of horizontal subgrade reaction k_h is known. An expression has been proposed by Davisson (1970), and adopted by Prakash and Sharma (1990), for the estimation of the modulus of horizontal subgrade reaction

$$k_h = 67 s_u \tag{11}$$

where s_u=undrained shear strength of the cohesive soil. The undrained shear strength may be determined from laboratory testing of soil samples, or estimated from in situ tests such as cone penetrometer tests. As a guide, however, Table 1 provides a correlation between the consistency and undrained shear strength of the cohesive soil (Das 1990). It should also be noted that the modulus of horizontal subgrade reaction, as estimated using Eq. (11) and Table 1, corresponds to the working load level. Such a value tends to overestimate the lateral stiffness of the soil-pile system when evaluating the yield displacement of the extended pile-shaft. The argument for reducing the modulus of horizontal subgrade reaction is presented together with the cohesionless soil in the next section.

Table 1. Undrained Shear Strength of Cohesive Soils [adapted from Das (1990)]

Estimated consistency	Undrained shear strength s_u (kN/m^2)
Very soft	<12
Soft	12–25
Firm	25–50
Stiff	50–100
Very Stiff	100–200
Hard	>200

Equivalent Depth-to-Fixity: Cohesionless Soils

For an elastic pile embedded in a cohesionless soil, the lateral stiffness of the soil is commonly modeled with an elastic Winkler foundation with a linearly increasing modulus of horizontal subgrade reaction. For a long pile, i.e., embedment length greater than four times the characteristic length R_n [defined later in Eq. (14)], the lateral displacement Δ_g and rotation θ_g of the pile at the ground level are given by (Poulos and Davis 1980)

$$\Delta_g = \frac{V}{EI_e}[2.40R_n^3 + 1.60R_n^2 L_a] \tag{12}$$

$$\theta_g = \frac{V}{EI_e}[1.60R_n^2 + 1.74R_n L_a] \tag{13}$$

where R_n=characteristic length of the pile and is given by

$$R_n = \sqrt[5]{\frac{EI_e}{n_h}} \tag{14}$$

and n_h=rate of increase of modulus of horizontal subgrade reaction in unit of force/length.[3]

$$n_h = \frac{k_h}{z} \tag{15}$$

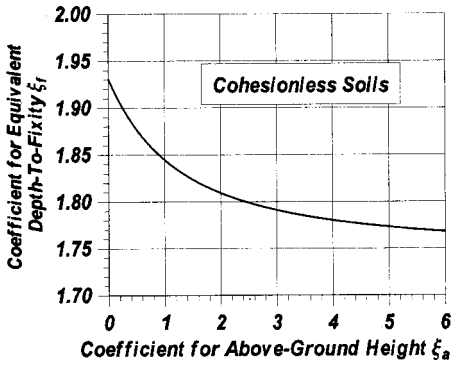

Fig. 4. Coefficient for equivalent depth-to-fixity of cohesionless soils

Similar to the approach taken for cohesive soils, the above-ground height L_a and equivalent depth-to-fixity L_f can be defined in terms of the characteristic length R_n, i.e., $L_a \equiv \xi_a R_n$ and $L_f \equiv \xi_f R_n$. The lateral stiffness of the soil-pile system can thus be written as

$$K_{sp} \equiv \frac{V}{\Delta} = \frac{EI_e}{R_n^3} \frac{1}{[2.4+3.2\xi_a+1.74\xi_a^2+\xi_a^3/3]} \tag{16}$$

By equating the lateral stiffness of the soil-pile system K_{sp} from Eq. (16) to the lateral stiffness of the equivalent cantilever K_c from Eq. (1), the coefficient for equivalent depth-to-fixity is

$$\xi_f = \sqrt[3]{7.2+9.6\xi_a+5.22\xi_a^2+\xi_a^3} - \xi_a \tag{17}$$

Fig. 4 shows the variation of the coefficient for equivalent depth-to-fixity for $0 \leqslant \xi_a \leqslant 6$. For a lateral force applied at the ground level, i.e., $\xi_a = 0$, the coefficient for equivalent depth-to-fixity is $\xi_f = 1.93$. The coefficient for equivalent depth-to-fixity decreases rapidly with increase in aboveground height for small values of ξ_a, similar to that observed for cohesive soils. For an above-ground height in the range of $2 < \xi_a < 6$, the coefficient for equivalent depth-to-fixity varies between 1.81 and 1.77. The relatively small variation of ξ_f also led to an approximate expression by Scarlat (1996) for free-head piles embedded in cohesionless soils

$$L_f = 1.8R_n \quad \text{if } L_a/R_n \geqslant 1 \tag{18}$$

$$= 2.2R_n \quad \text{if } L_a/R_n < 1 \tag{19}$$

Eq. (18) was also suggested by Davisson (1970) earlier for $L_a/R_n \geqslant 1$.

The equivalent depth-to-fixity L_f for piles embedded in a cohesionless soil can be determined if the lateral stiffness of the soil, as characterized by the rate of increase of the modulus of horizontal subgrade reaction n_h, is known. Guidance for the selection of n_h is currently available in the literature. For example, Fig. 5, which has been reproduced from ATC-32 (1996), provides a plot of n_h and effective friction angle ϕ as a function of the relative density of the soil for both dry and submerged sands. The value of n_h in Fig. 5, however, is typically estimated at the working load level, which may be as low as 1/4 of the ultimate load. The definition of yield limit state, on the other hand, should be based on first yielding of the longitudinal reinforcement of the pile. At the first-yield limit state of the pile, the inelastic deformation of the soil will be significantly larger than that at the working load level, resulting in a much smaller secant stiffness. This means that the appropriate value of n_h for lateral strength and ductility assessment of piles is much smaller than that given in Fig. 5. Ex-

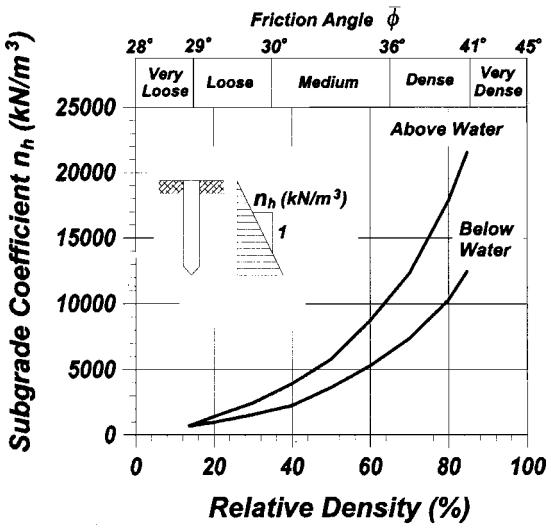

Fig. 5. Subgrade coefficient and effective friction angle of cohesionless soils (ATC-32 1996)

perimental results presented in the companion paper (Chai and Hutchinson 2002) indicated that the value of n_h could be as low as 1/5 of that shown in Fig. 5. Although the equivalent depth-to-fixity is not very sensitive to the variation of large n_h, a smaller value of n_h nonetheless results in a 20% or more increase in the equivalent depth-to-fixity. As noted in the previous section, a similar reduction should be made for the modulus of horizontal subgrade reaction of cohesive soils, even though experimental results are currently not available for such soils.

Inelastic Soil-Pile System

In using the equivalent fixed-base cantilever model for assessing the ductility capacity of a yielding pile-shaft, it must be recognized that the maximum bending moment does not occur at the base of the cantilever but at a depth above the equivalent depth-to-fixity. The depth-to-maximum-moment defines the location of the in-ground plastic hinge and will influence the lateral strength and ductility capacity of the pile. The depth-to-maximum-moment, however, depends on the ultimate resistance of the soil and the flexural strength of the pile, and will be considered separately for cohesive and cohesionless soils in the next two sections.

Depth-to-Maximum-Moment: Cohesive Soils

Extensive studies have been conducted in the past to quantify the ultimate soil pressure distribution acting on a laterally loaded pile. For a purely cohesive soil, the ultimate soil pressure was found to increase from about $2s_u$ at the ground level to a stress level between 8 and $12s_u$ at a depth of about $3D$ (Broms 1964a), where s_u=undrained shear strength of the cohesive soil and D=pile diameter. The ultimate soil pressure was found to remain fairly constant beyond a depth of $3D$. A simplified soil pressure was subsequently proposed by Broms (1964a) where zero soil pressure was assumed between the ground level and depth of $1.5D$, followed by a constant soil pressure of $9s_u$ to the depth-of-maximum-moment. The simplified soil pressure distribution, which is shown in Fig. 6(a), is similar to the rectangular stress block used for calculating the ultimate flexural strength of reinforced concrete sections (ACI 1999).

For stiff cohesive soils, however, large lateral resistance is developed in the upper region of the soil, resulting in the forma-

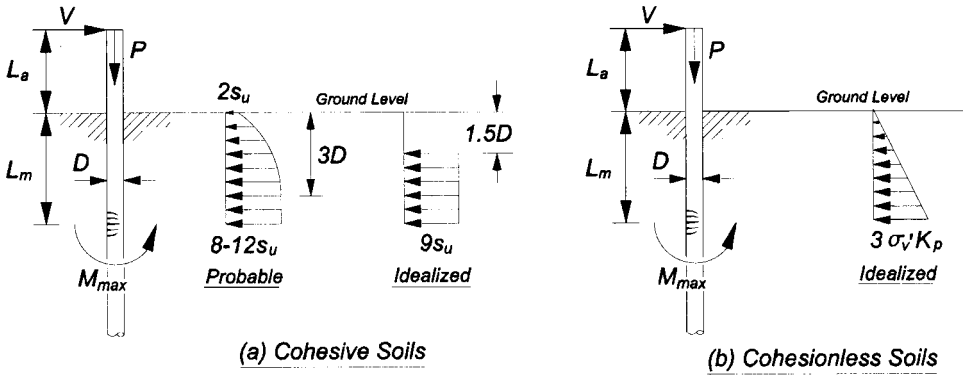

Fig. 6. Ultimate soil pressure distributions of laterally loaded piles

tion of the plastic hinge close to the ground surface. The simplified soil pressure distribution by Broms (1964a), on the other hand, does not lend itself to the formation of a plastic hinge for a depth less than $1.5D$. Consequently, the rectangular soil pressure distribution tends to underestimate the lateral strength of the soil-pile system for stiff cohesive soils. In this paper, a parabolic distribution of ultimate soil pressure is assumed for the upper region, followed by a constant soil pressure at greater depth. In equation form, the ultimate soil pressure distribution is given by

$$p_u(z)=\begin{cases}\dfrac{1}{27}s_u\left[54+84\dfrac{z}{D}-7\left(\dfrac{z}{D}\right)^2\right] & \text{for } z\leqslant 6D\\ 11.3s_u & \text{for } z>6D\end{cases} \tag{20}$$

where z=depth below the ground surface. Eq. (20) assumes an ultimate soil pressure of $2s_u$ at the ground level, a soil pressure of $9s_u$ and $11.3s_u$ at depths of $3D$ and $6D$, respectively, and a constant pressure of $11.3s_u$ for a depth greater than $6D$. For most cases, however, the depth-to-maximum-moment is less than $6D$ except for very soft clay, which means that the constant soil pressure of $11.3s_u$ for $z>6D$ is often not needed for the calculation.

The depth-to-maximum-moment as well as the ultimate lateral force resisted by the pile can be determined using the parabolic soil pressure distribution. The equilibrium of horizontal forces and bending moments requires

$$V_u=\int_0^{L_m}p_u(z)Ddz \tag{21}$$

$$M_{\max}=V_u(L_a+L_m)-\int_0^{L_m}p_u(z)D(L_m-z)dz \tag{22}$$

where V_u=ultimate lateral force and $M_{\max}$=flexural strength of the pile. Eqs. (21) and (22) can be integrated and rearranged into

$$M^*_{\max}=2L^*_aL^*_m+(1+\tfrac{14}{9}L^*_a)L^{*2}_m+\tfrac{7}{81}(12-L^*_a)L^{*3}_m-\tfrac{7}{108}L^{*4}_m \quad \text{for } L^*_m\leqslant 6 \tag{23}$$

$$V^*_u=2L^*_m+\tfrac{14}{9}L^{*2}_m-\tfrac{7}{81}L^{*3}_m \quad \text{for } L^*_m\leqslant 6 \tag{24}$$

where $V^*_u=V_u/s_uD^2$=normalized lateral strength of the soil-pile system; $M^*_{\max}=M_{\max}/s_uD^3$=normalized flexural strength of the pile; $L^*_a=L_a/D$=normalized aboveground height; and $L^*_m=L_m/D$=normalized depth-to-maximum-moment. The normalized depth-to-maximum-moment, as given by the solution of Eq. (23), is shown in Fig. 7 for $M^*_{\max}=0$–300 and for $L^*_a=0-10$. It can be seen from Fig. 7 that for very stiff cohesive soils, i.e., small value of $M^*_{\max}$, the normalized depth-to-maximum-moment may be less than 1.5. Thus the simplified soil pressure distribution by Broms (1964a) is inappropriate for stiff cohesive soils.

Depth-to-Maximum-Moment: Cohesionless Soils

The depth-to-maximum-moment for piles embedded in a cohesionless soil can be determined in a manner similar to that for cohesive soils by assuming an ultimate soil pressure distribution. In this paper, the depth-to-maximum-moment and ultimate lateral force resisted by the pile will be derived using the ultimate soil pressure distribution proposed by Broms (1964b) for cohesionless soils, which assumes that (i) the lateral displacement of the pile is large enough to fully mobilize the lateral resistance of the soil, (ii) the net soil pressure distribution on the pile is equal to C times the Rankine passive pressure, and (iii) the shape of the pile section does not influence the distribution of the ultimate soil resistance. Thus, according to assumption (ii), the net soil pressure acting on the pile may be assumed to be a linear function of the depth z and be written as

$$p_u(z)=C\sigma'_v(z)K_p \tag{25}$$

where σ'_v=vertical effective overburden stress and may be taken as the effective unit weight of the soil γ' times the depth z and K_p=passive soil pressure coefficient of the cohesionless soil and is given by

$$K_p=\frac{1+\sin(\bar{\phi})}{1-\sin(\phi)} \tag{26}$$

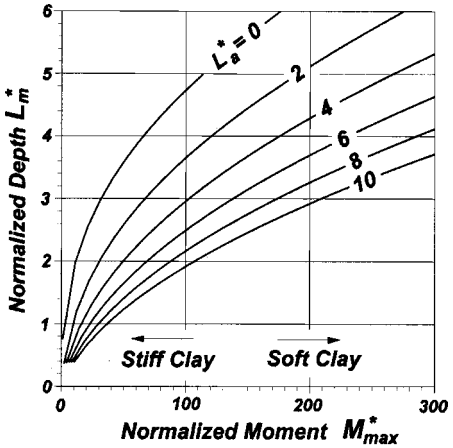

Fig. 7. Normalized depth-to-maximum-moment of cohesive soils

where $\bar{\phi}$=effective friction angle. Using the condition of zero shear force at the section of maximum bending moment, the equilibrium of horizontal forces requires

$$L_m = \sqrt{\frac{2V_u}{CK_p\gamma' D}} \tag{27}$$

The summation of bending moments about the section of maximum bending moment requires

$$M_{\max} = V_u L_a + \sqrt{\frac{8V_u^3}{9CK_p\gamma' D}} \tag{28}$$

Eqs. (27) and (28) can be solved simultaneously to give the normalized depth-to-maximum-moment

$$L_m^* = \frac{1}{2}\left[\frac{(L_a^*)^2}{p} - L_a^* + p\right] \tag{29}$$

where

$$p = \sqrt[3]{\frac{12}{C}M_{\max}^* - (L_a^*)^3 + \sqrt{\frac{24}{C}M_{\max}^*\left(\frac{6}{C}M_{\max}^* - (L_a^*)^3\right)}} \tag{30}$$

and the normalized lateral strength of the soil-pile system

$$V_u^* = \frac{C}{2}(L_m^*)^2 \tag{31}$$

where $M_{\max}^* = M_{\max}/K_p\gamma' D^4$=normalized flexural strength and $V_u^* = V_u/K_p\gamma' D^3$=normalized lateral strength. In the original work by Broms (1964b) the coefficient C was assumed to be 3, and this value may be adopted for the flexural strength and ductility assessment of a yielding pile-shaft. Note that care must be taken when evaluating Eqs. (29) and (30), as the parameter p in Eq. (30) may be a complex number depending on the values of $M_{\max}^*$ and L_a^*. The normalized depth-to-maximum-moment L_m^* in Eq. (29), however, should be a real number. For the special case of $M_{\max}^*=0$, there are three roots for the parameter p, namely $-L_a^*$, $(0.5+0.866i)L_a^*$, and $(0.5-0.866i)L_a^*$, where $i=\sqrt{-1}$. The use of the first root, i.e., $p=-L_a^*$, results in a negative value of $L_m^*=-3/2L_a^*$, which is incorrect. However, the choice of the second or third roots, i.e., $p=(0.5\pm 0.866i)L_a^*$, gives rise to $L_m^*=0$, and hence the correct value for the normalized lateral strength, i.e., $V_u^*=0$, according to Eq. (31). Even though the special case of $M_{\max}^*=0$ has no practical significance, it nonetheless illustrates the need to pay attention to the selection of roots for the solution.

Kinematic Relation for Ductility Demand

The equivalent fixed-base cantilever model may be used to estimate the local curvature ductility demand of a yielding pile-shaft. A kinematic relation between the displacement ductility factor μ_Δ and curvature ductility factor μ_ϕ can be developed by assuming a concentrated plastic hinge rotation at the location of maximum bending moment as shown in Fig. 2. The plastic displacement Δ_p at the top of the pile can be written as

$$\Delta_p = \theta_p(L_a + L_m) \tag{32}$$

where θ_p=plastic hinge rotation. Since the plastic rotation can be replaced by

$$\theta_p = (\phi - \phi_y)L_p \quad \text{for } \phi \geq \phi_y \tag{33}$$

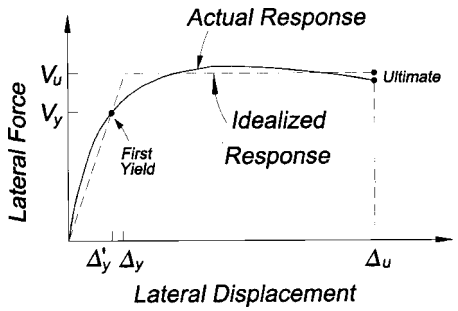

Fig. 8. Actual and idealized elastoplastic lateral force-displacement responses

where ϕ, ϕ_y=curvature and equivalent elastoplastic yield curvature, respectively, and L_p=equivalent plastic hinge length, the plastic displacement in Eq. (32) becomes

$$\Delta_p = L_p(\phi - \phi_y)(L_a + L_m) \tag{34}$$

By defining the normalized length as before, i.e., $L_a^* \equiv L_a/D$ and $L_m^* \equiv L_m/D$, and the normalized plastic hinge length $\lambda_p \equiv L_p/D$, Eq. (34) becomes

$$\Delta_p = \lambda_p(\phi - \phi_y)(L_a^* + L_m^*)D^2 \tag{35}$$

For an idealized elastoplastic response shown in Fig. 8, the ultimate lateral force V_u is related to the equivalent elastoplastic yield displacement Δ_y by

$$V_u = \frac{3EI_e}{(L_a^* + L_f^*)^3 D^3}\Delta_y \tag{36}$$

The ultimate lateral force V_u, however, may be written in terms of the maximum moment $M_{\max}$:

$$V_u = \frac{M_{\max}}{M_{\max}^* D}V_u^* \tag{37}$$

where V_u^* and $M_{\max}^*$ are the normalized lateral strength and normalized flexural strength, respectively, which have been defined earlier for cohesive and cohesionless soils. By equating Eqs. (36) and (37), the equivalent elastoplastic yield displacement can be written as

$$\Delta_y = \frac{M_{\max}}{EI_e}\frac{(L_a^* + L_f^*)^3 V_u^*}{3M_{\max}^*}D^2 \tag{38}$$

Since the equivalent elastoplastic yield curvature ϕ_y is given by

$$\phi_y = \frac{M_{\max}}{EI_e} \tag{39}$$

the equivalent elastoplastic yield displacement Δ_y may be written as

$$\Delta_y = \frac{\phi_y}{3}\frac{(L_a^* + L_f^*)^3 V_u^* D^2}{M_{\max}^*} \tag{40}$$

By substituting the elastoplastic yield displacement Δ_y from Eq. (40) into Eq. (32), and by defining the displacement ductility factor μ_Δ as

$$\mu_\Delta \equiv \frac{\Delta_u}{\Delta_y} = 1 + \frac{\Delta_p}{\Delta_y} \tag{41}$$

a kinematic relation between the displacement ductility factor μ_Δ and curvature ductility factor μ_ϕ may be obtained

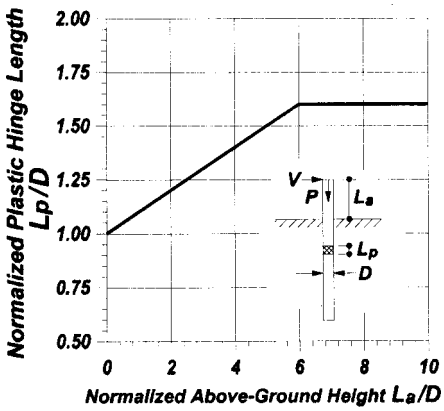

Fig. 9. Assumed equivalent plastic hinge length of concrete piles

$$\mu_\Delta = 1 + 3\lambda_p(\mu_\phi - 1)\frac{(L_a^* + L_m^*)}{(L_a^* + L_f^*)^3}\frac{M_{\max}^*}{V_u^*} \tag{42}$$

where curvature ductility factor $\mu_\phi \equiv \phi/\phi_y \geq 1$. It can be seen from Eq. (42) that the kinematic relation depends on the aboveground height, the equivalent depth-to-fixity, the depth-to-maximum-moment, and the plastic hinge length of the pile. The accuracy of the kinematic model is compared with experimental data in the companion paper (Chai and Hutchinson 2002).

The curvature ductility demand in the plastic hinge region of a yielding pile-shaft can be estimated if the equivalent plastic hinge length of the pile is known. A study by Budek et al. (2000) for piles embedded in cohesionless soils, and adopted by Priestley et al. (1996), showed that the plastic hinge length varies with the lateral stiffness of the soil and aboveground height of the pile. Experimental results (Chai and Hutchinson 2002), however, showed that the plastic hinge length was rather insensitive to the lateral stiffness of the soil, and depends primarily on the aboveground height L_a. Experimental plastic hinge lengths of about $1.2D$ and $1.6D$ were obtained for aboveground heights of $L_a = 2D$ and $6D$, respectively. In this paper, the equivalent plastic hinge length is assumed to increase linearly with the aboveground height from $1.0D$ at the ground level to $1.6D$ at an aboveground height of $L_a = 6D$. For an aboveground height greater than $6D$, a constant plastic hinge length of $L_p = 1.6D$ is assumed. The proposed variation of plastic hinge length with aboveground height is shown in Fig. 9.

Examples

To illustrate the use of the proposed kinematic model, consider the bridge structure shown in Fig. 10 for two different soil conditions: (i) soft clay and (ii) medium dry sand. The bridge structure is supported on an extended pile-shaft with a diameter of $D = 1.83$ m, an aboveground height of $L_a = 8.89$ m, and an embedded length of $L = 19.8$ m. The following structural parameters are assumed for the analysis: (i) expected concrete compressive strength, as suggested by ATC-32 (1996), $f'_{ce} = 1.3f'c = 44.8$ MPa, (ii) expected yield strength of the longitudinal and transverse steel, as suggested by ATC-32 (1996), $f_{ye} = 1.1f_y = 455.1$ MPa, (iii) elastic modulus of the concrete $E_c = 31{,}685$ MPa, (iv) axial force $P = 4528$ kN (axial load ratio of $P/f'_{ce}A_g = 0.038$), (v) longitudinal reinforcement $= 52\Phi$ 36 ($d_b = 36$ mm; longitudinal area ratio of $\rho_l = 0.02$), and (vi) transverse reinforcement $= \Phi$ 19 spiral at a pitch of 76 mm ($d_b = 19$ mm; confining steel ratio of $\rho_s = 0.0089$). A concrete cover of 75 mm is assumed for the transverse spiral of the pile. The flexural rigidity of the cracked pile section, estimated from a moment-curvature analysis using the first-yield limit state of the section, is $EI_e = 6.97 \times 10^6$ kN m^2. The simulated and idealized elastoplastic moment-curvature responses of the pile section are shown in Fig. 11. The idealized elastoplastic response has been obtained by equating the area under the nonlinear moment-curvature curve to the area under the idealized elastoplastic curve. In this case, the ultimate moment of the idealized elastoplastic response is $M_{\max} = 21{,}320$ kN m while the equivalent elastoplastic yield curvature is $\phi_y = 0.00306$ rad/m. The ultimate curvature of the pile section, based on the ultimate compressive strain of the confined concrete, is $\phi_u = 0.04467$ rad/m. Thus the elastoplastic curvature ductility capacity of the pile section is $(\mu_\phi)_{\text{cap}} = 14.6$. The curvature ductility demand will be determined for a displacement ductility factor of $\mu_\Delta = 3$, as assumed by ATC-32 (1996) for seismic design of extended pile-shafts.

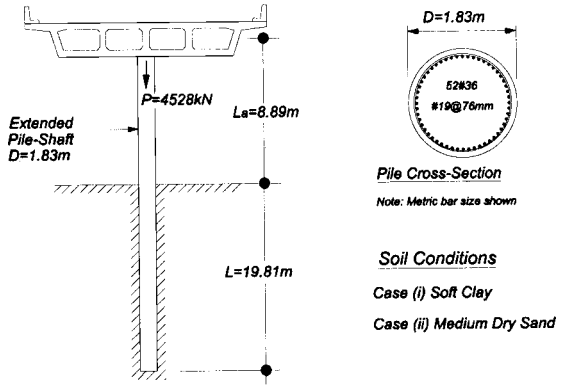

Fig. 10. Example bridge structure supported on extended pile-shafts

Case (i): Soft Clay

It is assumed that the undrained shear strength of the soft clay, as estimated from Table 1, is $s_u = 20$ kN/m^2. The modulus of horizontal subgrade reaction is $k_h = 1340$ kN/m^2 from Eq. (11). Even though it was noted earlier that the modulus of horizontal subgrade reaction should be reduced when assessing the flexural strength and ductility of piles, the value of k_h is not reduced in this example due to a lack of experimental data for cohesive soils. The characteristic length of the pile is $R_c = 8.49$ m from Eq. (4). Substituting the coefficient for aboveground height ξ_a

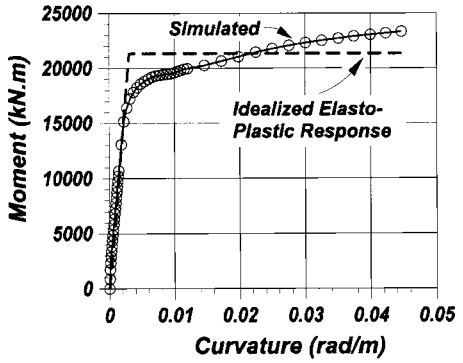

Fig. 11. Moment-curvature response of pile-shaft

$=8.89/8.49=1.05$ into Eq. (8), the coefficient for equivalent depth-to-fixity is $\xi_f=1.49$, giving the equivalent depth-to-fixity $L_f=12.65$ m or corresponding to a normalized equivalent depth-to-fixity of $L_f^*=12.65/1.83=6.9$.

The depth-to-maximum-moment, which is smaller than the equivalent depth-to-fixity, is estimated from the normalized flexural strength of the pile, i.e., $M_{\max}^*=M_{\max}/s_uD^3=173.9$. Substituting $M_{\max}^*=173.9$ and $L_a^*=8.89/1.83=4.86$ into Eq. (23), the normalized depth-to-maximum-moment is $L_m^*=3.72$, or corresponding to a depth-to-maximum-moment of $L_m=6.81$ m. The normalized lateral strength from Eq. (24) is $V_u^*=24.55$, giving a lateral strength of $V_u=1642$ kN.

The curvature ductility demand in the plastic hinge is calculated using the plastic hinge length interpolated from Fig. 9. Using $L_a^*=4.86$, the normalized plastic hinge length is estimated to be $\lambda_p=1.48$, or corresponding to a plastic hinge length of $L_p=2.71$ m. Substituting $\mu_\Delta=3$, $L_f^*=6.9$, $L_m^*=3.72$, $L_a^*=4.86$, $\lambda_p=1.48$, $M_{\max}^*=173.9$, and $V_u^*=24.55$ into Eq. (42), the local curvature ductility demand is $(\mu_\phi)_{\text{dem}}=13.1$, which is close to the curvature ductility capacity of the pile $(\mu_\phi)_{\text{cap}}=14.6$. Note that the local curvature ductility demand is sensitive to the lateral stiffness of the soil. A reduction of the modulus of horizontal subgrade reaction by a factor of 2 would increase the curvature ductility demand to 17.8, which then exceeds the ductility capacity of the pile. The relative sensitivity of local ductility demand to soil stiffness illustrates to need to better quantify the appropriate level of reduction for k_h of cohesive soils.

Case (ii): Medium Dry Sand

The same bridge structure is analyzed for a medium dry sand where the rate of increase of modulus of horizontal subgrade reaction for an effective friction angle of $\phi=33°$ is $n_h=6{,}000$ kN/m^3 (estimated from Fig. 5). However, based on pile tests in cohesionless soils (Chai and Hutchinson 2002), the value of n_h is reduced by a factor of 4 to 1,500 kN/m^3 in this example. An effective unit weight of $\gamma'=17.5$ kN/m^3 is assumed for the dry sand. The characteristic length of the pile is $R_n=5.41$ m from Eq. (14). Substituting the coefficient for aboveground height $\xi_a=8.89/5.41=1.64$ into Eq. (17), the coefficient for depth-to-fixity is $\xi_f=1.82$ giving an equivalent depth-to-fixity $L_f=9.85$ m, or corresponding to a normalized equivalent depth-to-fixity of $L_f^*=9.85/1.83=5.38$.

In calculating the depth-to-maximum-moment, the passive soil pressure coefficient from Eq. (26) is $K_p=3.39$, giving a normalized flexural strength of $M_{\max}^*=M_{\max}/K_p\gamma'D^4=32.0$. Assuming a value of $C=3$ and substituting $M_{\max}^*=32.0$ and $L_a^*=4.86$ into Eqs. (29) and (30), the normalized depth-to-maximum-moment is $L_m^*=1.87$, or corresponding to a depth-to-maximum-moment of $L_m=3.42$ m. The normalized lateral strength is $V_u^*=5.25$ from Eq. (31), or corresponding to an ultimate lateral force of $V_u=1{,}908$ kN.

Since the aboveground height is the same for both cases, the same plastic hinge length of $L_p=2.71$ m is used. Substituting $\mu_\Delta=3$, $L_f^*=5.38$, $L_m^*=1.87$, $L_a^*=4.86$, $\lambda_p=1.48$, $M_{\max}^*=32.0$, and $V_u^*=5.25$ into Eq. (42), the local curvature ductility demand is $(\mu_\phi)_{\text{dem}}=12.8$, which is less than the curvature ductility capacity of the pile $(\mu_\phi)_{\text{cap}}=14.6$. Thus the bridge structure supported by the extended pile-shaft in medium dry sand is also expected to have adequate ductility capacity. A comparison between case (i) and case (ii) indicates that, for a given displacement ductility factor, the curvature ductility demand increases with decreasing stiffness of the soil.

Conclusions

An analytical model suitable for assessing the lateral strength and ductility demand of a yielding pile-shaft is developed in this paper. The model, based on an extension of the commonly used equivalent fixed-base cantilever model, uses different depths to estimate the lateral stiffness and strength of the soil-pile system. The lateral stiffness of the soil-pile system is characterized in terms of an equivalent depth-to-fixity, which is derived from the elastic solution of piles embedded in an elastic Winkler foundation. For lateral strength calculation, however, the depth-to-maximum-moment is assumed to occur at a depth above the depth-to-fixity and is calculated using the flexural strength of the pile and the ultimate pressure distribution of the soil. By assuming a concentrated plastic hinge rotation at the depth-to-maximum-moment, a kinematic model relating the local curvature ductility demand to the global displacement ductility demand of the soil-pile system is derived. The kinematic relation indicates that the curvature ductility demand depends on the aboveground height, depth-to-maximum-moment, depth-to-fixity, and equivalent plastic hinge length. The analytical model, which is fairly easy to use and suitable for design purposes, is illustrated using a bridge structure supported on an extended pile-shaft embedded in cohesive and cohesionless soils. A comparison between the model and experimental data is made in a companion paper.

Acknowledgments

The research described in this paper was funded by Caltrans under Contract No. 59Y500 with Mr. Thomas Sardo as the Contract Monitor and Mr. Timothy Leahy as the Contract Manager. Their financial support is gratefully acknowledged. Comments and suggestions by Tara C. Hutchinson of UC Irvine and Ross W. Boulanger of UC Davis are appreciated. Any opinions, findings, and conclusions expressed in the paper are those of the writer and do not necessarily reflect the view of the sponsor.

References

American Concrete Institute. ACI. (1999). ''Building code requirements for reinforced concrete and commentary.'' *ACI 318-99/R-99*, Farmington Hills, Mich.

Applied Technology Council ATC-32. (1996). *Improved seismic design criteria for California bridges: provisional recommendations*, Redwood City, Calif.

Broms, B. B. (1964a). ''Lateral resistance of piles in cohesive soils.'' *J. Soil Mech. Found. Div., Am. Soc. Civ. Eng.* 90(SM2), 27–63.

Broms, B. B. (1964b). ''Lateral resistance of piles in cohesionless soils.'' *J. Soil Mech. Found. Div., Am. Soc. Civ. Eng.* 90(SM3), 123–156.

Budek, A. M., Priestley, M. J. N., and Benzoni, G. (2000). ''Inelastic seismic response of bridge drilled-shaft RC pile/columns.'' *J. Struct. Eng.*, 126(4), 510–517.

Caltrans (1986). ''Bridge design specifications manual.'' Calif. Dept. of Trans., Sacramento, Calif.

Chai, Y. H., and Hutchinson, T. C. (2002). ''Flexural strength and ductility of extended pile-shafts. II: Experimental study.'' *J. Struct. Eng.*, 128(5), 595–602.

Chapman, H. E. (1995). ''Earthquake resistant bridges and associated highway structures: current New Zealand practice.'' *Proc., National*

Seismic Conf. on Bridges and Highways, San Diego, sponsored by Federal Highway Administration, Washington, D.C. and California Dept. of Transportation, Sacramento, Calif.
Das, B. M. (1990). *Principles of geotechnical engineering*, 2nd Ed., PWS-Kent., Boston.
Davisson, M. T. (1970). ''Lateral load capacity of piles.'' Highway Research Record, No. 333, 104–112.
Dowrick, D. J. (1987). *Earthquake resistant design*, 2nd Ed., Wiley-Interscience, New York.
Park, R. (1998). ''New Zealand practice on the design of bridges for earthquake resistance.'' T160-1, *Proc., 1st Structural Engineers World Congress*, San Francisco, Elsevier Science, New York.
Pender, M. J. (1993). ''Aseismic pile foundation design analysis.'' *Bull. New Zealand Natl. Soc. Earthquake Eng.*, 26(1), 49–160.
Poulos, H. G., and Davis, E. H. (1980). *Pile foundation analysis and design*, Wiley, New York.
Prakash, S., and Sharma, H. D. (1990). *Pile foundations in engineering practice*, Wiley-Interscience, New York.
Priestley, M. J. N., Seible, F., and Calvi, G. M. (1996). *Seismic design and retrofit of bridges*, Wiley-Interscience, New York.
Scarlat, A. S. (1996). *Approximate methods in structural seismic design*, 1st Ed., E & FN SPON, London.